International Journal of Innovative Technology and Exploring Engineering (IJITEE)
ISSN: 2278-3075 (Online), Volume-9 Issue-5, March 2020

Computational Modeling on Heat Transfer Enhancement and Fluid Flow Behavior of Al_2O_3-Water Nanofluid through a Circular Duct

Prakash Ghose, Kunja Bihari Sahu, Ajay Kumar Sahu

Abstract*: *In this work, heat transfer behaviour from a isothermal-walled micro channel has been investigated by using Al_2O_3-water nanofluid as working fluid. A computational simulation has been carried out for high Reynolds number flow, having different volume fraction of nanoparticles added to it such as; 0%, 1%, 4% and 6%. It has been observed that the properties such as; density, thermal conductivity and viscosity increase with increase in nanoparticles. On the other hand, with increase in the volume fraction of nanoparticles, the specific heat decreases. It also has been observed that the heat transfer from the hot wall increases with Reynolds number and addition of nanoparticles to the nanofluid as well. The friction factor for the flow system decreases with increase the Reynolds number, but for different nanofluids its value is very much closer to each other. With increase in volume fraction of nanoparticles, the pumping power increases. Moreover, with increase in Reynolds number, pumping power increases.

Keywords: Al_2O_3-water nanofluid, heat transfer, pumping power

I. INTRODUCTION

To design various thermal systems, generally used in industries such as heat exchangers, cooling of electronic chips, solar thermal power plant etc., a precise heat transfer analysis must be required. Heat transfer is a phenomenon by which temperature of a system can be maintained according to the physical necessity. Convective heat transfer is affected passively by varying flow geometry, boundary conditions or by changing the thermal conductivity of the base fluid. In a convection process, amount of heat transfer is limited for a particular fluid due to its thermo physical properties. Therefore, for few decades of twentieth century, heat transfer through nanofluids becomes the centre of attraction for many researchers. Application of nanofluid is currently considered as one of the best method for heat transfer enhancement where certain amount of metal particles of better thermal conductivity is suspended through a base fluid. Since water is the cheapest liquid available, water based nanofluids are generally used in various applications. However, chemically stable metals, metal oxides or carbon in various forms are typically used as nanoparticles. Water based Al_2O_3 nanofluid is the most popular and used widely in engineering applications for cheaper in price and better performance as well. In order to study the convective heat transfer performance of nanofluid, computational modelling now becomes a reliable tool in the field of engineering. Both single phase and multiphase approach are used for the simulation. In multiphase approach, both the base fluid and nanoparticles are taken as separate phases where as in single phase approach the nanoparticles-suspended nanofluid is considered as a single fluid. Rashidi et al. [1] investigated both the approaches and observed that the multiphase model predictions is little significant in the temperature field, while there is no much significance in the hydrodynamic field. Seyf et al. [2] studied the augmentation of heat transfer by using Al_2O_3-water nanofluid and CuO-water nanofluid. They found better heat transfer in case of Al_2O_3-water nanofluid when the particle diameter is less. Sharifi et al. [3] solved a single phase model considering the temperature dependent properties of Al_2O_3-EG water nanofluid. It has been observed that, with increase in water percentage in base fluid, heat transfer increases. Moreover, the heat transfer increases with increase in particle volume fraction and Reynolds number. Roy et al. [4] concluded that the conventional fluid like water is one of the best fluids for base fluid where even the addition of small amount of Al_2O_3 enhances the heat transfer rate. Sasmito et al. [5] recommended strongly using Al_2O_3 rather than CuO due to its better performance. However it has also been suggested that too much of increase in nanoparticles increases pumping power. Nguyen et al. [6] used Al_2O_3 nanofluid for electronic chip cooling. It has been observed that 6.8 percent volume fraction of nanoparticles with water gives highest heat transfer coefficient..

In this work, we studied the enhancement of heat transfer by using Al_2O_3 nanoparticles with a wide range of volume fraction added in base fluid taken as water through a micro channel at very high Reynolds number flow. The entire problem has been analyzed by using CFD technique and the parameters have been calculated such as Nusselt number and friction factor to study the hydrodynamic and thermal behaviour of the flow.

Revised Manuscript Received on March 30, 2020.
***** Correspondence Author
Prakash Ghose, School of Mechanical Engineering, KIIT University, Bhubaneswar, India. Email: pghosefme@kiit.ac.in
Kunja Bihari Sahu*, School of Mechanical Engineering, KIIT Deemed to be University, Bhubaneswar, India. Email: kbsahu@yahoo.com.
Ajay Kumar Sahu, School of Mechanical Engineering, KIIT University, Bhubaneswar, India. Email: sahu.ajay93@gmail.com

II. PHYSICAL MODEL AND COMPUTATIONAL MODELING

Fig. 1 shows the physical model of the axi-symmetric channel with constant cross-section. In two dimensional forms, the computational domain of the channel of circular cross section is represented by a rectangle, as displayed. The diameter of 0.0005m and the length of 0.1m have been taken respectively.

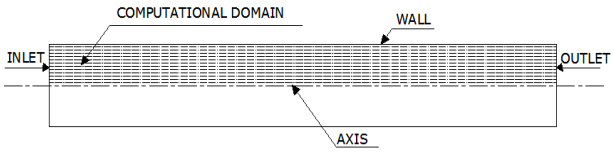

Fig. 1 Physical geometry and computational model

A. Boundary Conditions

No slip boundary conditions are considered for the wall surfaces, which are non-porous for which both the velocity components are set to zero. A constant wall temperature (350 K) is taken for the channel wall. Axi-symmetry boundary condition was assigned at centerline. Velocity inlet boundary condition for inlet boundary and pressure outlet condition at outlet have been specified. Simulation has been conducted with four different Reynolds number such as 20000, 40000, 60000 and 80000. Reynolds number is defined as $\mathrm{Re} = \frac{\rho v D}{\mu}$, where ρ is the density and μ is the viscosity of nano fluid calculated from the correlations given in the following sections and D is the diameter of the channel. A constant inlet temperature (290 K) was assigned at the channel inlet. The operating pressure is used as atmospheric pressure (1.01235 bar). Inlet turbulent intensity and length scale has been calculated by using the empirical correlations given as [7]:

$$I = \frac{U'}{U_{avg}} = 0.16\left(\mathrm{Re}_{Ds}\right)^{-1/8} \quad (1)$$

$$l = 0.07 D_s \quad (2)$$

B. Governing equations

In this work the suspended nanoparticles are assumed to be well dispersed throughout the base fluid. Therefore single phase approach has been considered for solving the governing equations in Eulerian frame. The slip velocity between base fluid and nanoparticles are assumed to be negligible. The equation given as follows for conservation of mass, or continuity equation, is solved with the help of CFD software Ansys Fluent 14.0.

Conservation of mass

$$\frac{\partial}{\partial x_i}\left(\rho \bar{u}_i\right) = 0 \quad (3)$$

Conservation of momentum

$$\frac{\partial}{\partial x_i}\left(\rho \bar{u}_i \bar{u}_j\right) = -\frac{\partial \bar{p}}{\partial x_i} + \frac{\partial}{\partial x_j}\left(\bar{\tau}_{ij} - \rho \overline{u_i' u_j'}\right) \quad (4)$$

conservation of energy

$$\frac{\partial}{\partial x_i}\left(\rho \bar{u}_i \bar{h}\right) = \frac{\partial}{\partial x_i}\left(\frac{\mu}{\sigma}\frac{\partial \bar{h}}{\partial x_i} - \rho \overline{h' u'_i}\right) + S_E \quad (5)$$

where, $\bar{u}_i$ and $\bar{p}$ are the time average mean flow velocity and time average mean pressure. The stress tensor in the momentum equation is expressed as $\bar{\tau}_{ij}\left(= \mu\left(\frac{\partial \bar{u}_i}{\partial x_j} + \frac{\partial \bar{u}_j}{\partial x_i}\right)\right)$. $-\rho \overline{u_i' u_j'}$ is the Reynolds stress and it is an additional term that has been formed due to time averaging. The Reynolds stresses in the momentum equation is expressed as the product of turbulent viscosity (μ_t) and the fluid strain in terms of the mean velocities.

In the two equation k-ε model of turbulence, the turbulent viscosity is expressed in terms of turbulent kinetic energy (k) and its dissipation rate (ε). The two turbulence quantities are evaluated by solving the respective conservation equations. In the standard k-ε model [8], the k and ε equations are expressed as follows:

$$\frac{\partial}{\partial x_i}\left(\rho k u_i\right) = \frac{\partial}{\partial x_j}\left[\left(\mu + \frac{\mu_t}{\sigma_k}\right)\frac{\partial k}{\partial x_j}\right] + G_k - \rho\varepsilon \quad (6)$$

$$\frac{\partial}{\partial x_i}\left(\rho \varepsilon u_i\right) = \frac{\partial}{\partial x_j}\left[\left(\mu + \frac{\mu_t}{\sigma_\varepsilon}\right)\frac{\partial \varepsilon}{\partial x_j}\right] + C_{1\varepsilon}\frac{\varepsilon}{k}G_k - C_{2\varepsilon}\rho\frac{\varepsilon^2}{k} \quad (7)$$

In the above equations, G_k represents the generation of turbulent kinetic energy, which is expressed in terms of the mean velocity values as,

$$G_k = \mu_t\left(\frac{\partial u_i}{\partial x_j} + \frac{\partial u_j}{\partial x_i}\right)\frac{\partial u_i}{\partial x_j} \quad (8)$$

The turbulent viscosity is computed by combining k and ε values as, $\mu_t = C_\mu \rho \frac{k^2}{\varepsilon}$, where, C_μ is a constant having a value of 0.09. The model constants $C_{1\varepsilon}$, $C_{2\varepsilon}$, σ_k and σ_ε in the k and ε equations have default values obtained empirically [9].

C. Method of solution

In this study, the solution of the flow field has been obtained by solving the conservation equations of Reynolds averaged mass and momentum for a steady, axi-symmetric case within the computational domain numerically. The gravity effect has been neglected. A pressure correction based iterative SIMPLE algorithm with second order upwind scheme is used in the specified solver in Ansys Fluent for discretizing the convective transport terms. The convergence criteria are specified as 10^{-4} for all the dependent variables except for the energy equation that has been specified as 10^{-6}. The default values of under-relaxation factor are used in the simulation work.

D. Thermophysical properties of nanofluid

In this work, temperature independent properties are used to determine the thermo-physical properties of the nanofluid.

The correlation given in following equation is used to calculate the specific heat which is frequently used by various authors for Al_2O_3-water nanofluid [10-12].

$$Cp_{nf} = (1-\phi)Cp_{bf} + \phi Cp_p \quad (9)$$

A well validated Pak and Cho model [10] given in following equation is used to determine the density of water based Al_2O_3 nanofluid.

This model is used by various researchers [12-14] in their simulation work to analyze the heat transfer behavior of Al_2O_3-water nanofluid.

$$\rho_{nf} = (1-\phi)\rho_{bf} + \phi\rho_p \quad (10)$$

Viscosity is an important fluid property that largely affects the flow field. The correlation proposed by Maiga et al. [12] is used by different researchers to study the flow and heat transfer behaviour by using Al_2O_3-water nanofluid as coolant [15, 16]. The correlation for viscosity without considering the Brownian motion is expressed as:

$$\mu_r = \frac{\mu_{nf}}{\mu_{bf}} = 123\phi^2 + 7.3\phi + 1 \quad (11)$$

Thermal conductivity is the vital physical property of nanofluid that is majorly responsible to determine the heat transfer capacity of a fluid. For thermal conductivity of Al_2O_3-water nanofluid at various nanoparticle volume fractions, the correlation developed by Maxwell [17] is used. Moreover, this model is used by various authors in their research works [18, 19]. The expression is given as:

$$\frac{k_{nf}}{k_{bf}} = \frac{k_p + 2k_{bf} - 2\phi(k_{bf} - k_p)}{k_p + 2k_{bf} + \phi(k_{bf} - k_p)} \quad (12)$$

Where ρ represents the density, C_p represents the specific heat, μ represents the viscosity and k represents the thermal conductivity. The subscripts *bf*, *p* and *nf* stands for base fluid, nanoparticles and nanofluid respectively whereas φ is the volume fraction of nanoparticles. The physical properties of Al_2O_3 nanofluid at different nanoparticles volume fractions are given in Table-1.

Table 1 Physical Properties of Al_2O_3 nanofluid

Volume Fraction of nanoparticles	ρ (kg/m^3)	μ (Ns/m^2)	K (W/mK)	C_p (J/kg K)
0%	998.2	9.93 x 10^{-5}	0.597	4182
1%	1027.1	1.07 x 10^{-4}	0.613	4147
4%	1113.4	1.47 x 10^{-4}	0.666	4045
6%	1171.1	1.86 x 10^{-4}	0.705	3977

E. Calculation of physical parameters

The convective heat transfer of a system is represented by the two important parameters, namely convective heat transfer coefficient and Nusselt number. Average Nusselt number has been calculated by using the following equation as: $Nu = \frac{hD}{k}$, where h is the convective heat transfer coefficient and calculated from the basic equation for convection $\frac{Q}{A} = h(T_w - T_b)$. Wall heat flux is obtained from the simulated result. The bulk mean temperature T_b is calculated as $T_b = \left(\frac{T_{in} + T_{out}}{2}\right)$ where, T_{out} is the mass weighted average at pipe outlet. The friction factor (f) for the flow system has been evaluated by using the Darcy Weisbach formulation which is expressed as: $h_l = \frac{fLv^2}{2gD}$, where L is the length of the pipe, v is the average velocity at inlet, g is the acceleration due to gravity, D is the pipe diameter, f is the friction factor and h_l is the head loss due to friction. h_l has been evaluated as: $h_l = \frac{p_{out} - p_{in}}{\rho g}$. Pumping power is calculate as: Pumping Power = ($p_{in} - p_{out}$) × discharge, where, p_{out} and p_{in} are the mass weighted average pressure at outlet and inlet respectively.

III. RESULTS AND DISCUSSION

A. Grid independence test and model validation

The entire grid independence test has been carried out by using three different grid sizes such as 25 × 250, 50 × 500 and 100 × 1000 with structured grid. In Fig. 2, axial velocity at the centre line of the pipe has been drawn. Just near the inlet, the axial velocity is same for all the grid sizes taken whereas at the fully developed region the result is closer for grid sizes of 50 × 500 and 100 × 1000 whereas the difference in the result is appreciable for grid size of 25 × 250. Therefore the grid size of 50 × 500 has been adopted for simulation to evaluate the results considering computational economy.

The simulated average Nusselt number has been compared with the experimental values obtained by Pak-Cho. Fig. 3 shows the validation for nanofluid with 4% volume fraction of Al_2O_3. The deviation is somewhat higher at lower Reynolds number, but the result is moderately validated at higher Reynolds number. However, the variation trend of Nusselt number with respect to Reynolds number is similar with Pak-Cho and it has been validated moderately.

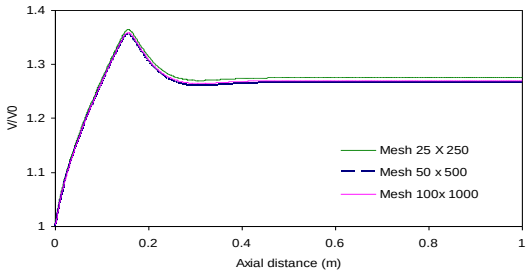

Fig. 2 Axial velocity at axis for Re = 20000 and nanoparticles volume fraction 4%

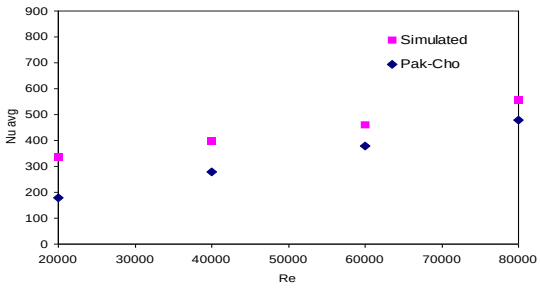

Fig. 3 Comparison of simulated average Nusselt number at various Reynolds number for 4% nanoparticles in nanofluid

B. Effect of Reynolds number on various flow and thermal parameters

Fig. 4 depicts the distribution of non dimensional axial velocity along the axis for various Reynolds number for 4% volume fraction of Al_2O_3 in water. In Y-axis, 'v' represents the velocity inside the flow field and 'v_o' represents the velocity at inlet. It is shown that the axial velocity gradually increases from the inlet to some distance towards the downstream. Due to the boundary layer growth around the pipe, fluid is being retarded within the boundary layer region. Therefore, in order to satisfy the continuity the axial velocity towards the centre gradually increases. However, within the fully developed region velocity remains constant up to the exit. The profile of axial velocity at the centre line shows a spike just before the starting of fully developed region unlike for the laminar flow. In turbulent flow, the turbulent intensity at the inlet is same throughout the inlet region. But at the downstream, the turbulent intensity becomes highest at the conjunction of boundary layers which is the starting of the fully developed region on the centre line. This causes an increased in axial velocity in order to compensate the radial velocity decrement which is shown as a spike at this region.

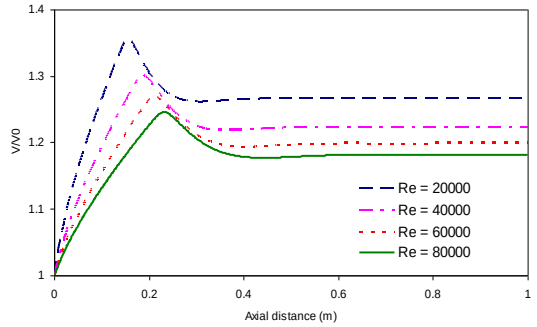

Fig. 4 Axial velocity along the for 4% volume fraction of nanoparticles in nanofluid at various Reynolds number

Moreover, it has been observed that the axial velocity at the centre line for low Reynolds number flow is higher throughout the length of the channel as compared to higher Reynolds number flow. With the higher velocity for higher Reynolds number, the boundary layer thickness becomes smaller and the effect of viscous resistance is limited to certain height. Therefore, the profile of axial velocity in radial direction become more uniform and the axial velocity becomes less for higher Reynolds number to satisfy the continuity theory.

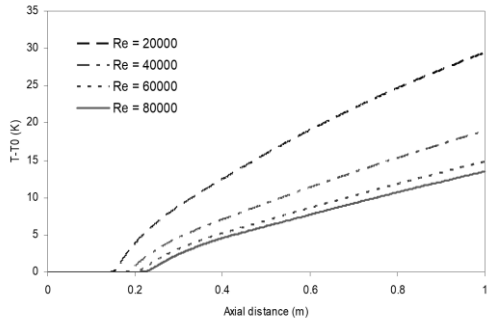

Fig. 5 Temperature along the axis for 4% volume fraction of nanoparticles in nanofluid at various Reynolds number

Fig. 5 presents the bulk temperature of the nanofluid along the tube axis for ϕ = 4% at different Reynolds numbers. Up to certain length along the axis, the axial temperature remains same as the inlet temperature. It is because; the thermal boundary layer thickness is very small in this entrance region. As a result the heat from the wall is not being transferred into this region. After a certain distance along the axis the temperature increases along with the axis as the heat release from the wall is continuously added to the fluid up to the exit.

Moreover, from Fig. 5, it has been observed that the temperature along the axis is higher in case of low Reynolds number flow than high Reynolds number flow. The flow with low velocity creates a thicker hydrodynamic boundary layer with a deprived velocity gradient. As a result, low Reynolds number flow causes a poor convective heat transfer that keeps a higher temperature along the axis.

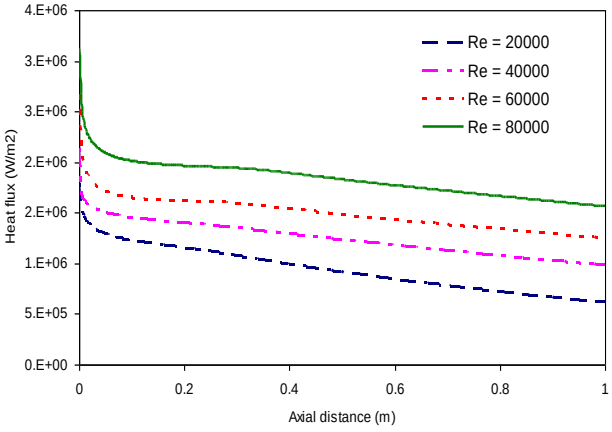

Fig. 6 Wall heat flux for 4% volume fraction of nanoparticles in nanofluid at various Reynolds number

Fig. 6 shows the variation of heat flux along the channel wall. The wall heat flux at the inlet is the maximum. It is obvious that the fluid at the entrance is having the lowest temperature. Therefore, maximum amount of heat from the wall is conducted into the fluid due to highest temperature difference in between wall and fluid at entrance region. That causes a higher wall heat flux at the entrance. At the downstream, the fluid temperature increases by taking heat from the wall continuously up to the exit.

Therefore, due to lower temperature difference in between wall and fluid along the downstream, less amount of heat is transferred from the wall. That causes a lower wall heat flux along the downstream.

It is observed from the Fig. 6 that at higher Reynolds number flow, wall heat flux is always higher all along the wall as compared to low Reynolds number flow. Because at higher Reynolds number flow, higher velocity of fluid near the wall takes the heat out at a higher rate. Therefore, in order to maintain a constant wall temperature a larger amount of heat is required to be transferred from the wall. That causes a higher wall heat flux in this case.

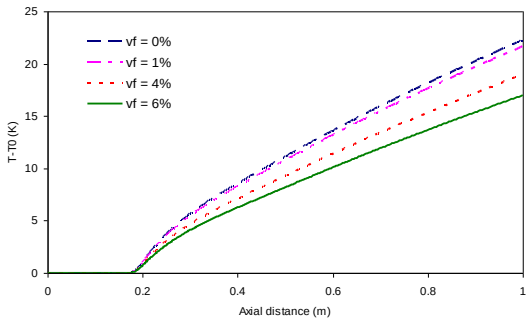

Fig. 7 Temperature along the axis for various volume fraction of nanoparticles in nanofluid at Re=40000

Fig. 7 depicts the effect of temperature along axis with various volume fractions of nanoparticles at Reynolds number of 40000. It is a well known phenomenon that, heat transfer from the wall towards the centerline becomes more for the fluid with greater volume fraction of particles due to better diffusion of heat energy. But for same Reynolds number the calculated inlet velocity is higher due to change in fluid properties with the addition of particles. With higher volume fraction of nanoparticles, the kinematic viscosity of the nanofluid increases. For a given Reynolds number, the inlet velocity is higher for higher volume fraction of nanoparticles. Therefore, the heat loss from the wall has been dominated by convection as compared to diffusion for higher volume fraction nanofluid due to high inlet velocity.

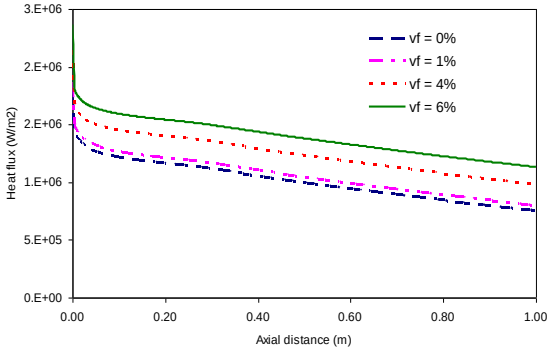

Fig. 8 Wall heat flux for various volume fraction of nanoparticles in nanofluid at Re=40000

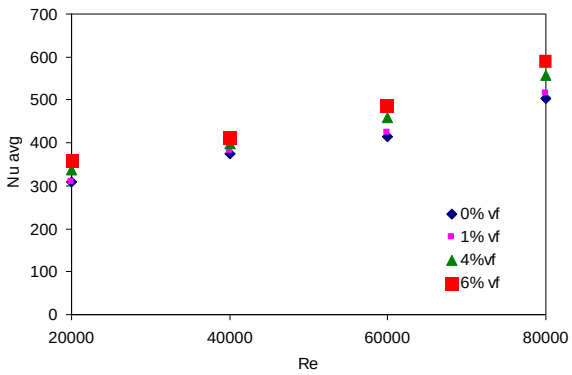

Fig. 9 Average Nusselt number at various volume fraction of nano particles for various Reynolds number flow

It has been seen that irrespective of axial location, the wall heat flux is more for higher volume fraction of nanoparticles as shown in Fig. 8. This implies that with the addition of nanoparticles, heat transfer increases. Therefore, the heat transfer coefficient is higher with the addition of more nanoparticles in the base fluid and the average Nusselt number is always higher for higher volume fraction of nanoparticles. This is evident from Fig. 9. As Reynolds number increases, the average Nusselt number also increases. This is because the fluid velocity increases with Reynolds number which in turn enhances the convective heat transfer.

C. Effect of Reynolds number and nanoparticles volume fraction on friction factor and pumping power

Friction factor is an important parameter due to which the major loss during the flow occurs. Fig. 10 depicts the friction factors at various Reynolds number for fluid having 4% volume fraction of nanoparticles. From this figure, it is observed that the trend of friction factor line for different Reynolds number fairly follows the Moody's curve. We have also calculated the friction factor for different Reynolds number for the fluid with various volume fractions of nanoparticles. Fig. 10 shows the variation of friction factor with Reynolds number for the volume fraction of 4%. It is observed that the friction factor decreases with increase in Reynolds number. However, it has been observed that the flow having fluid with higher fraction of nanoparticles is insignificantly higher than the flow having lower volume fraction nanofluid.

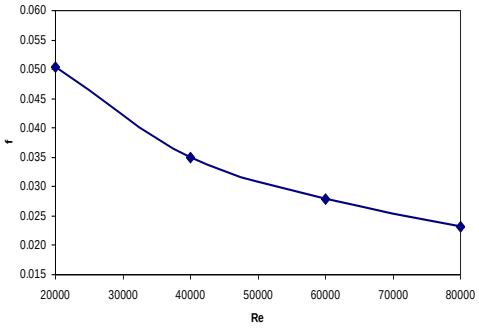

Fig. 10 Friction factor for various Reynolds number with 4% volume fraction of nanoparticles

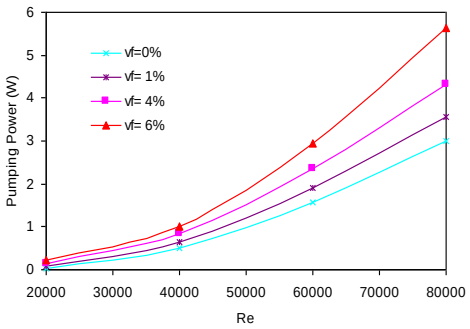

Fig. 11 Pumping power in watt for various Reynolds number with various volume fraction of nanoparticles in nanofluid

From Fig. 11, it has been observed that the pumping power increases with increase in Reynolds number irrespective of nanoparticles fraction present in nanofluid. The pumping power depends on the friction factor and the velocity of the fluid. The change in friction factor is negligible with increase in volume fraction, but the change in velocity is significant for the same volume fraction. The effect of change in velocity dominates the effect of change in friction factor. So, the pressure drop along the length of the tube is higher for higher Reynolds number as head loss due to friction becomes high as flow velocity increases. Therefore, more pumping power is needed to drive the fluid for higher Reynolds number flow. For this, viscosity plays a major role. As the viscosity of the fluid increases with increase in fraction of nanoparticles, it creates a higher resistance to the fluid flow. For the fluid flow having lower fraction of nanoparticles, less pumping power is required because smaller viscosity creates less resistance to flow.

IV. CONCLUSION

A numerical study has been conducted to study the flow and heat transfer behavior through a circular channel for various nanofluids with a wide range of Reynolds numbers. In this study, Al_2O_3–water nanofluid has been used to pass through a micro channel. Along with this, the effect of volume fraction such as 0%, 1%, 4% and 6% has been studied on heat transfer and fluid flow. The variation of axial velocity along the axis, wall heat flux, axial temperature, friction factor, pumping power as well as the important non dimensional number such as Nusselt number is also considered to analyze the thermo fluidic behavior of the flow system. It has been found that the temperature along the axis is high with lower Reynolds number and lower volume fraction of nanoparticles. As regard to properties, the density, thermal conductivity and viscosity increase with nanoparticles. However, specific heat decreases with increase in the nanoparticles volume fraction. The friction factor for the flow system decreases with increase in the Reynolds number but for different nanofluids, its value is very much closer to each other. With increase in volume fraction of nanoparticles, the pumping power increases. Moreover, with increase in Reynolds number, pumping power increases. Further, the Nusselt number increases with increase in Reynolds number or the volume fraction. Therefore, it is concluded that even though higher volume fraction increases the heat transfer rate, it needs more pumping work due to its high viscosity and density.

REFERENCES

1. M. Rashidi, A. Hosseini, I. Pop, S. Kumar, and N. Freidoonimehr, Comparative numerical study of single and two-phase models of nanofluid heat transfer in wavy channel, Applied Mathematics and Mechanics. 35 (2014) 831-848.
2. H. R. Seyf and M. Feizbakhshi, Computational analysis of nanofluid effects on convective heat transfer enhancement of micro-pin-fin heat sinks, International Journal of Thermal Sciences. 58 (2012) 168-179.
3. A. Sharifi, A. Emamzadeh, A. Hamidi, H. Farzaneh, and M. Rastgarpour, Computer-Aided simulation of heat transfer in nanofluids, in Proceedings of the International MultiConference of Engineers and Computer scientists, 2012.
4. G. Roy, C. T. Nguyen, and P.-R. Lajoie, Numerical investigation of laminar flow and heat transfer in a radial flow cooling system with the use of nanofluids, Superlattices and Microstructures. 35 (2004) 497-511.
5. A. P. Sasmito, J. C. Kurnia, and A. S. Mujumdar, Numerical evaluation of laminar heat transfer enhancement in nanofluid flow in coiled square tubes, Nanoscale research letters. 6 (2011) 376.
6. C. T. Nguyen, G. Roy, C. Gauthier, and N. Galanis, Heat transfer enhancement using Al_2O_3–water nanofluid for an electronic liquid cooling system, v Applied Thermal Engineering. 27 (2007) 1501-1506.
7. ANSYS fluent user's guide, release 14.0, 2011.
8. A. M. Abed, K. Sopian, H. Mohammed, M. Alghoul, M. H. Ruslan, S. Mat, and A. N. Al-Shamani, Enhance heat transfer in the channel with V-shaped wavy lower plate using liquid nanofluids, Case Studies in Thermal Engineering. 5 (2015) 13-23.
9. H. K. Versteeg and W. Malalasekera, An introduction to computational fluid dynamics: the finite volume method: Pearson education, 2007.
10. B. C. Pak and Y. I. Cho, Hydrodynamic and heat transfer study of dispersed fluids with submicron metallic oxide particles, Experimental Heat Transfer an International Journal. 11 (1998) 151-170.
11. Y. Xuan and Q. Li , Heat transfer enhancement of nanofluids, 21 (2000) 58-64.
12. S. E. B. Maiga, S. J. Palm, C. T. Nguyen, G. Roy, and N. Galanis, Heat transfer enhancement by using nanofluids in forced convection flows, International Journal of heat and fluid flow. 21 (2000) 58-64.
13. A. Akbarinia and A. Behzadmehr, Numerical study of laminar mixed convection of a nanofluid in horizontal curved tubes, Applied Thermal Engineering. 27 (2007) 1327-1337.
14. V. Bianco, F. Chiacchio, O. Manca, and S. Nardini, Numerical investigation of nanofluids forced convection in circular tubes, Applied Thermal Engineering. 29 (2009) 3632-3642.
15. S. Lee, S.-S. Choi, S. Li, and J. Eastman, Measuring thermal conductivity of fluids containing oxide nanoparticles, (1999) 280-289.
16. X. Wang, X. Xu, and S. U. Choi, Thermal conductivity of nanoparticle-fluid mixture, Journal of thermophysics and heat transfer. 13 (1999) 474-480.
17. M. Levin and M. Miller, Maxwell's treatise on electricity and magnetism, Uspekhi Fizicheskikh Nauk. 135 (1981) 425-440.
18. R. S. Vajjha and D. K. Das, Experimental determination of thermal conductivity of three nanofluids and development of new correlations, International Journal of Heat and Mass Transfer. 52 (2009) 4675-4682.
19. R. S. Vajjha, D. K. Das, and D. P. Kulkarni, Development of new correlations for convective heat transfer and friction factor in turbulent regime for nanofluids, International journal of heat and mass transfer. 53 (2010) 4607-4618.

AUTHORS PROFILE

Dr. Prakash Ghose received his Ph. D. degree from Jadavpur University, Kolkata. He has done his master degree from University College of Engineering, Burla, Odisha. Now he is working as Asst. Professor in KIIT Deemed to be University, Bhubaneswar. He published more than 16 articles in different journals and conferences. His research interest is Heat Transfer and Combustion.

Dr. Kunja Bihari Sahu is presently working as Professor in School of Mechanical Engineering, KIIT Deemed to be University, Bhubaneswar. He has accomplished his graduation and master degree in Mechanical Engineering from University College of Engineering, Burla, Odisha (presently, Veer Surendra Sai University of Technology) and Ph. D. degree from Jadavpur University, Kolkata. He has published more than 25 articles in different journals and conferences. He has supervised 3 Ph. D. and 15 M. Tech. students. His research interest is Heat Transfer and Combustion. He is a life member of Indian Society for Technical Education (ISTE), Indian Society for Heat and Mass Transfer (ISHMT), Indian Science Congress Association (ISCA). He is also a fellow of Institution of Engineers (India).

Mr. Ajay Kumar Sahu is a Ph. D. scholar working on solid fuel combustion. He received his master degree from University College of Engineering, Burla, Odisha.